

FULL SKY HARMONIC ANALYSIS HINTS AT LARGE ULTRA-HIGH ENERGY COSMIC RAY DEFLECTIONS

P. G. Tinyakov[*]***, F. R. Urban***[**]

Université Libre de Bruxelles, Service de Physique Théorique, CP225
1050, Brussels, Belgium

Received October 24, 2014

The full-sky multipole coefficients of the ultra-high energy cosmic ray (UHECR) flux have been measured for the first time by the Pierre Auger and Telescope Array collaborations using a joint data set with $E > 10$ EeV. We calculate these harmonic coefficients in the model where UHECR are protons and sources trace the local matter distribution, and compare our results with observations. We find that the expected power for low multipoles (dipole and quadrupole, in particular) is sytematically higher than in the data: the observed flux is too isotropic. We then investigate to which degree our predictions are influenced by UHECR deflections in the regular Galactic magnetic field. It turns out that the UHECR power spectrum coefficients C_ℓ are quite insensitive to the effects of the Galactic magnetic field, so it is unlikely that the discordance can be reconciled by tuning the Galactic magnetic field model. On the contrary, a sizeable fraction of uniformly distributed flux (representing for instance an admixture of heavy nuclei with considerably larger deflections) can bring simulations and observations to an accord.

Contribution for the JETP special issue in honor of V. A. Rubakov's 60th birthday

DOI: 10.7868/S0044451015030210

1. INTRODUCTION

Despite the fact that the actual sources of ultra-high energy cosmic rays (UHECRs) have still not been identified, it is rather natural to expect them to follow, to some extent, the large scale structure (LSS) observed in the sky. Indeed, the propagation distance of UHECRs of above 10^{19} eV is limited to several hundred megaparsecs due to their interaction with the intergalactic medium [1, 2]. The matter distribution is not homogeneous over such distances, hence if UHECRs are extragalactic, one expects an anisotropy in their arrival direction distribution, reflecting the inhomogeneity of the source distribution. Such anisotropies, on a sphere, can be revealed via a harmonic analysis, where the coefficients of the complete set of spherical harmonics carry the information, multipole by multipole, about the possibly nonuniform UHECR flux. The harmonic analysis is thus a way to compress the data in a form most suitable for statistical tests.

Recently the Telescope Array (TA) and Pierre Auger Observatory (PAO) collaborations have joined forces to provide the first full-sky UHECR map [3]. With single earth-based experiments being forcedly blind to a big chunk of the sky, only the combined data sets from two — or more — machines can provide the complete picture. This is particularly important for the harmonic analysis which, as detailed in the joint TA/PAO paper, strongly benefits from a whole sky coverage, both theoretically/qualitatively (no need to assume anything about the flux) and practically/quantitatively (some errors are significantly suppressed) [4]. Joining the data of the two experiments thus made possible, for the first time, to measure the harmonic multipoles of the UHECR flux distribution in an assumption-free way.

One natural question is then: is the harmonic power spectrum expected from the LSS the same as that actually observed? The caveat here is that UHECRs do not travel on a straight line from source to the Earth, because of the magnetic fields they encounter on their way; these deflect their trajectories and mask the original arrival directions, and with that the sources or UHECRs. The most relevant magnetic field in this re-

[*]E-mail: petr.tiniakov@ulb.ac.be
[**]E-mail: furban@ulb.ac.be

spect is housed by our own Galaxy (Galactic magnetic field, GMF), with strength in the microgauss range, see for instance [5] and references therein. The GMF is separated into large- (regular or coherent) and small- (turbulent or random) scale components, the regular part dominating the cosmic ray deflections. When combined, these fields are expected to steer 10 EeV protons by a few degrees, far away from the galactic plane, up to several tens of degrees at very low galactic latitudes. Now, what does this mean for the harmonic analysis? Are the anisotropies erased, or is the power spectrum distorted?

What we find in this analysis is that there is a striking mismatch between the power spectrum we simulate from the LSS, *assuming a purely protonic primary composition*, and the one reconstructed from the data: the amplitudes of low multipoles (particularly, the quadrupole C_2, the second momentum in the harmonic decomposition) in the data are significantly lower than the calculated LSS ones. The scope of this work is to delve deeper into this issue; in particular, we want to understand the role of the GMF in this result.

Before embarking on the analysis, we briefly summarise our findings.

• There is a lack of power in the low multipoles (notably, dipole and quadrupole) as observed by TA/PAO compared to the expectations from protons tracing LSS.

• The regular GMF shuffles direction-dependent single harmonic coefficients, demonstrating how these are not fully reliable indicators of source anisotropy.

• However, the power spectrum is barely affected by the regular GMF, which means that the latter can not bring observations and simulations to an accord.

• The random GMF has also very little effect on the low multipoles.

• A moderate fraction of uniformly-distributed events (which could, for instance, represent an admixture of heavy nuclei) instead does temper the tension between data and expectations, for it contributes to the isotropisation of the signal even on largest angular scales.

For the rest of the paper, we will begin summarising the results of the joint TA/PAO analysis in Sec. 2; then we will introduce the simulated power spectra from the LSS, and discuss the missing quadrupole problem in Sec. 3. The impact of the GMF on this result is detailed in Sec. 4, whereas the turbulent GMF is discussed in Sec. 5, alongside the effect on the power spectrum of a different composition of cosmic ray primaries. We will conclude in Sec. 6.

2. THE JOINT TA/PAO ANALYSIS

As any angular distribution on the unit sphere, the flux $\Phi(\mathbf{n})$ of cosmic rays in a given direction $\mathbf{n}$ can be decomposed in terms of a multipolar expansion onto the spherical harmonics $Y_{\ell m}(\mathbf{n})$:

$$\Phi(\mathbf{n}) = \sum_{\ell \geq 0} \sum_{m=-\ell}^{\ell} a_{\ell m} Y_{\ell m}(\mathbf{n}). \qquad (1)$$

Anisotropy fingerprints are encoded in the $a_{\ell m}$ multipoles. Nonzero amplitudes in the ℓ modes contribute in variations of the flux on an angular scales of about π/ℓ radians.

Cosmic ray events, in this language, are then simply sample points for the underlying sources distribution on the sphere. However, because the sky coverage is nonuniform, what these events are sampling is the flux times exposure distribution. Now, with full-sky but nonuniform coverage, the customary recipe [3] for decoupling directional exposure effects from anisotropy ones consists in weighting the observed angular distribution by the inverse of the *relative* directional exposure function $\varpi_r(\mathbf{n})$, so that, inverting Eq. (1), the actual data points are unbiassed estimators of the underlying flux:

$$\hat{a}_{\ell m} = \sum_{i=1}^{N} \frac{Y_{\ell m}(\mathbf{n}_i)}{\varpi_r(\mathbf{n}_i)}, \qquad (2)$$

where one can prove [3] that upon averaging over a large number of realisations one has $\langle \hat{a}_{\ell m} \rangle = a_{\ell m}$. Here N is the number of events, which are described as Dirac delta functions centred at the actual arrival directions $\mathbf{n}_i$.

While the individual $a_{\ell m}$ coefficients are direction-dependent, the angular power spectrum coefficients C_ℓ, defined as averages of $|a_{\ell m}|^2$ over m,

$$C_\ell = \frac{1}{2\ell + 1} \sum_{m=-\ell}^{\ell} |a_{\ell m}|^2 , \qquad (3)$$

are rotation-independent quantities. Given that the regular GMF results in a (direction-dependent) rotation of the events, one might expect that the power spectrum coefficients C_ℓ are much less sensitive to the presence of GMF than individual amplitudes $a_{\ell m}$.

Now, in order to achieve full-sky coverage, the data of two different experiments must be combined; hence, the total exposure has to be cross-calibrated in order to not introduce spurious effects in Eq. (2). The details of the cross-calibration procedure, and its performances, do not matter for us here, but can be found in Ref. [3] (see also [6, § 2]). Note, however, that in the cross-calibration procedure only a small subset of all events — those in the region of overlapping exposures — are used, and that the cross-calibration errors propagate mainly into the $m = 0$ components of the coefficients $a_{\ell m}$ (in equatorial coordinates).

The data sets used in the analysis consist of UHECRs with energies above 10 EeV, which amounts to 8259 for PAO, and 2130 for TA. The Table reports the results for the $a_{\ell m}$ coefficients as presented in the TA/PAO joint paper.

As one may see, there are no statistically significant deviations from isotropic expectation in any of the harmonic coefficients, the largest discrepancy being in the value of $a_{1,-1}$. One also observes that the errors are systematically larger for $m = 0$, particularly for the dipole $\ell = 1$: a consequence of the cross-calibration procedure.

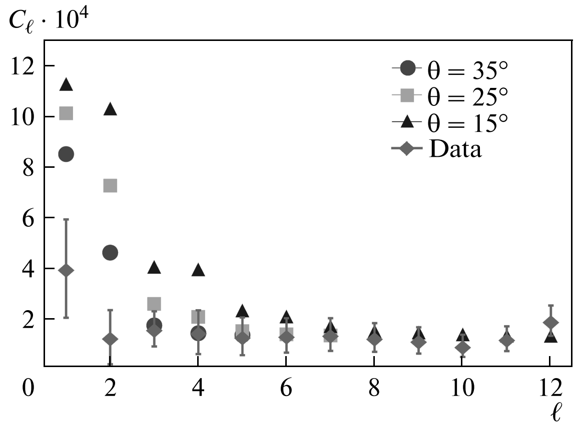

Fig. 1. The UHECRs angular power spectrum from the data and from simulated flux maps at different smearing angles, see the main text for details (color online see arXiv:1411.2486)

3. LARGE SCALE STRUCTURES AND ANISOTROPIES

In order to compare the power spectrum reconstructed from the data with the expectations from the LSS model, we need to build the flux map which we are going to sample with random Monte-Carlo events and derive expectations for the multipole coefficients. The procedure we used to build the expected flux is described in detail in [7, 8]. We first choose a galaxy catalogue, in this case the 2MASS Galaxy Redshift Catalog (XSCz) that is derived from the 2MASS Extended Source Catalog (XSC). The flux is calculated from the flux-limited subsample of galaxies with the apparent magnitude $m < 12.5$ at distances $D < 250$ Mpc by the method described in [7, 9, 10]. The contribution from beyond 250 Mpc is considered uniform. All galaxies are assumed to have the same intrinsic luminosity in UHECR. To determine their individual contributions to the total flux, we propagate protons to the Earth taking full account of the redshift, distance and attenuation effects. Individual fluxes are then smeared with a Gaussian distribution of an angular width θ, which is a free parameter. This is done to account for limited detector resolution, and, most importantly, the effects of the regular and turbulent GMF. In this Section, we will not attempt to reconstruct the original direction of the events through the coherent GMF, which is instead investigated in detail in Sec. 4. Finally, where this is relevant, the flux map is weighted accounting for the non-uniform exposure of the actual experiment (or experiments).

With the map of the expected flux on Earth at hand, we simulate random sets of cosmic ray events that this flux distribution would produce. Each mock set has the same number of events as the actual data. We then calculate the harmonic coefficients and the power spectrum for each of these mock sets. For each harmonic coefficient, we determine the mean value and the variance; we generate as many mock sets as is necessary to make the variances negligible. In Fig. 1, we show the result of this procedure: orange diamonds are the actual data points with their errors; blue triangles, green boxes, and red circles are the expectations from the simulations with smearing angles of $\theta = 15°$, $25°$, $35°$, respectively[1)].

The most striking feature of this plot is the considerable tension between the power in the low multipoles (notably, the dipole and quadrupole) expected from the galaxy distribution, and what is observed in the data, the predicted power being systematically higher. With a smearing angle of 15°, both the dipole and quadrupole components of the flux are expected to vary at the level of $\sim 10\,\%$, while no flux variations are detected in the data. However, because the dipole measurement has larger error, the discrepancy is most prominent in the case of the quadrupole. As the smearing angle grows, the expected flux variation is watered down, the larger the multipole number, the faster the isotropy sets in.

---

1) Smearing the flux with a given ϑ by definition wipes away any power for multipoles $\ell \gtrsim \pi/\vartheta$, so we do not include multipoles for which by construction there is no power.

Table. Dipole, quadrupole, and octupole moments, with their uncertainties, in equatorial coordinates. These are normalized so that the $a_{\ell m}$ measure the relative deviation with respect to the monopole a_{00}, that is, the $a_{\ell m}$ are redefined such that $a_{\ell m} \to \sqrt{4\pi} a_{\ell m}/a_{00}$

ℓ	m	$a_{\ell m}$	ℓ	m	$a_{\ell m}$	ℓ	m	$a_{\ell m}$
							-3	-0.022 ± 0.034
				-2	0.038 ± 0.035		-2	0.030 ± 0.039
	-1	-0.102 ± 0.036		-1	0.067 ± 0.040		-1	0.067 ± 0.037
1	0	0.006 ± 0.074	2	0	0.017 ± 0.042	3	0	-0.027 ± 0.040
	1	-0.001 ± 0.036		1	0.004 ± 0.040		1	0.009 ± 0.037
				2	0.040 ± 0.035		2	-0.004 ± 0.039
							3	-0.011 ± 0.034
$C_1 = 0.0035 \pm 0.0024$			$C_2 = 0.0016 \pm 0.0014$			$C_3 = 0.00097 \pm 0.00088$		

All the higher multipoles are more or less within their expected values in the LSS case, although at the level of precision currently attainable with TA and PAO, these are difficult to distinguish from simple isotropy. We will devote the rest of the paper to discuss this observation, and to understand and clarify the role of the GMF in drawing conclusions from it.

A comment is in order at this point. As we have seen, the measurement of the power spectrum coefficients C_ℓ, in particular C_1, is obscured by the cross-calibration procedure which introduces a large error. One may define observables that are free from this problem (note that, as we will argue in the next section, such observables would also lose an important advantage of C_ℓ: their insensitivity to the regular magnetic field). These are the coefficients c_n of the Fourier decomposition of the flux in right ascension ϕ defined as follows,

$$c_n \equiv \frac{1}{2} \int d\mathbf{n}\, \Phi(\mathbf{n}) Y_n(\phi),$$

with $Y_n(\phi) \equiv (\sqrt{2}\cos n\phi, 1, \sqrt{2}\sin|n|\phi)/\sqrt{2\pi}$ for $n > 0$, $n = 0$, and $n < 0$, respectively. The coefficients c_n can be measured in a single experiment without making any assumption about the flux. They are obviously free from the errors introduced by the cross-calibration procedure[2)].

In order to make contact with previously defined quantities, we note that c_n can be expressed in terms of spherical harmonic coefficients $a_{\ell m}$ with $\ell \geq |n|$ (see Appendix for a derivation). So, we may use the harmonic coefficients $a_{\ell m}$ calculated above for the LSS model to infer the LSS prediction for c_n. The two lowest coefficients $c_{\pm 1}$ receive contributions from the projection of the dipole and of odd ℓ higher multipoles onto the right ascension plane. For the LSS model, the contribution of the dipole is dominant, and we may approximately write

$$\begin{aligned} c_{+1} &\approx \frac{\sqrt{3}\pi}{8} a_{1,-1}, \\ c_{-1} &\approx \frac{\sqrt{3}\pi}{8} a_{1,1}. \end{aligned} \tag{4}$$

In order to compare to the measurements, the coefficients (4) can be combined into an amplitude $d^2 \equiv (c_{-1}^2 + c_{+1}^2)/2$ and a phase $\alpha \equiv \arctan(c_{-1}/c_{+1})$. For a smearing angle of 15°, the LSS model predicts $d = 0.0226$ and $\alpha = 73°$, which has to be compared to $d = 0.0138 \pm 0.0049$ and $\alpha = 89° \pm 20°$, obtained from the joint data set of [3]. Notice that the incompatibility with the LSS models worsens when we include the z component to form C_1, despite the fact that the largest error comes with $a_{1,0}$; this is because the data value for $a_{1,0}$ is very small compared to that of the LSS model — the latter is within a factor of 3 from the other dipole coefficients.

The relations (4) become exact if the flux contains only a dipole and any other even multipole, but has zero power for all odd $\ell > 1$; in this approximation, these coefficients have also been measured by the Pierre Auger collaboration alone [11, 12] — in this case, the errors on these quantities are indeed smaller: the price to pay is a *a priori* decision on what the flux should be.

[2)] Although it is indeed possible to determine these coefficients univocally from a single experiments, it is not guaranteed that in the north and south hemisphere they will agree with each other.

4. THE GMF AND THE HARMONIC MULTIPOLES

The results of the previous section did not take the effects of the propagation of UHECRs through the GMF into account directly, but only indirectly through a variable, and relatively large, smearing angle. A better approximation is to treat the regular part of GMF explicitly and leave the smearing to represent the random deflections only, deflections which can amount to about $10°$ to $20°$ for our 10 EeV protons, see [13, 14]. So one may wonder whether the regular GMF could wipe away, or distort, any anisotropic harmonic imprint, for example by transferring power from a multipole to another. A caveat here is that the regular GMF is not known well enough for accurate predictions of $a_{\ell m}$.

We will show, however, that while the direction-dependent $a_{\ell m}$ are indeed quite sensitive to the strength (and shape) of the magnetic field in the Milky Way, the direction-blind power spectrum C_ℓ is quite stable against these perturbations.

In order to demonstrate this empirically, we adopted the model of [15] for the regular GMF, and we simulated again the expected fluxes from the LSS, now propagating the flux through the GMF. This GMF model has two components, a disk field and a halo field, with independent strengths. We chose to work with the best-fit parameters as reported in [15] for the version dubbed bisymmetric spiral structure, or BSS: this means that the overall disk and halo strengths are $B_{disk} = 2\ \mu$G and $B_{halo} = 4\ \mu$G, respectively. We should stress, however, that neither the choice of the model parameters, nor the model itself has too strong impact on our results, as what we found is that the effect of GMF on the coefficients of the power spectrum is small.

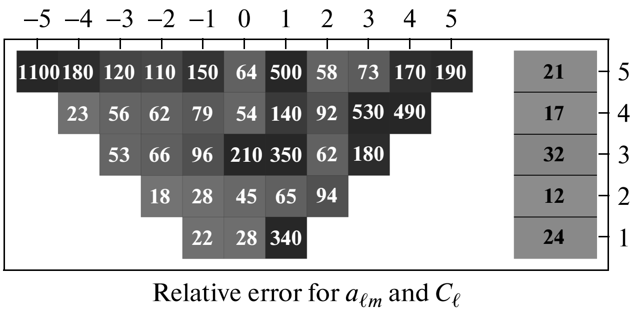

Fig. 2. Color-coded relative variation of the $a_{\ell m}$ and the C_ℓ with varying magnetic field strength (in percent) (color online see arXiv:1411.2486)

To assess the variability, or sensitivity, of the harmonic coefficients and power spectrum on the strength of the GMF — a similar virtual experiment can be performed by changing its shape, or both — we generated 1000 fluxes[3)] with randomly chosen field strengths ranging from zero to twice the best fit values, that is $0 \leq B_{disk} \leq 4\,\mu$G and $0 \leq B_{halo} \leq 8\,\mu$G. Since each time the reconstructed flux will be slightly different, we show the relative percent variation (standard deviations over the mean: σ_x/mean_x, where x stands for the $a_{\ell m}$ and C_ℓ) in Fig. 2. We immediately notice that the average spread for some harmonic coefficients $a_{\ell m}$ is much larger than that of the power spectrum coefficients C_ℓ, proving our point above. We show in the picture only multipoles up to $\ell = 5$, but we performed the same exercise for multipoles up to $\ell = 20$, and obtained the same result.

A legitimate doubt is that since we do not expect these distributions to be Gaussian, as we are not sampling the same sky many times with different randomly generated events, a very skewed distribution may bias this result and the standard deviations would not represent the actual excursion of the quantities under observation. For example, the spread of the C_ℓ might be a bad indicator of how much the power spectrum actually varies, but be accurate in describing the fluctuations of $a_{\ell m}$. We have checked that the ratio between the total excursion for a given parameter, that is, its maximum minus its minimum, versus the corresponding deviation, $|\max x - \min x|/\sigma_x$, is more or less the same (to within 15 %) for all the quantities we analyse, which means that for both the $a_{\ell m}$ and the C_ℓ coefficients, the spread is an equally good descriptor of the range which these parameters can attain.

The conclusion we draw from these tests is that:

- the power spectrum is a much more suitable quantity in assessing the anisotropic properties of the UHECR flux when dealing with the GMF, as it is much more robust against the details (still poorly known) of the GMF itself, compared to the direction-dependent $a_{\ell m}$;
- the absolute power spectrum itself is not much affected quantitatively by the regular GMF: we thus believe it is unlikely that the reason behind the low quadrupole observed in the data is to be found in the effect of GMF UHECRs deflections.

3) When propagating UHECRs through the magnetic field, we use monochromatic primaries, since the deviations are maximised at the lowest energy, for simplicity.

5. ISOTROPIC FRACTION AND THE HARMONIC MULTIPOLES

So far, we have always worked with proton primaries, but the UHECRs composition at the highest energies is not known. If instead of protons we were to propagate iron nuclei, the deflections they endure would be a factor 26 larger, due to the corresponding larger rigidity. We thence expect that a fraction of iron or other nuclei in the total UHECR flux, because of its tendency to isotropise, would help loosening the tension between the observed and simulated multipoles.

To assess this, we again generated several flux maps where we subtract a fraction of the total proton flux and replace it with an isotropic one, to roughly simulate the contribution of iron. We vary this "iron fraction" (essentially, the isotropic fraction) between zero and one, and recalculate the power spectrum for each map; we then compare with the data and their errors, and compute the statistical significance of the low ℓ coefficients of the power spectrum in each map. Were the primaries a mix of several different elements, the LSS predictions would fall in between the values we obtain below.

In Fig. 3, we show 1σ, 2σ, 3σ, etc, contours for the dipole C_1, quadrupole C_2, and octupole C_3, where in addition to varying isotropic fraction, we also change the smearing angle of the map, to account for a variable turbulent GMF strength.

We can perform this test with or without the regular GMF, and the results, according to our previous section, should not change much; this is indeed the case, as Fig. 4 shows: the curves move down by approximately 1σ, which again does not suffice to resolve the tension between data and LSS expectations.

As we see, both the dipole and the quadrupole in the data prefer a more isotropic Universe, with the quadrupole being the most pronouncedly incompatible with the expectations from LSS.

Correlating the arrival directions of UHECRs with LSS is a logical surmise, so this result is somewhat puzzling; however, it is not completely unexpected, as at this energy it is known that, for example, the TA data alone prefer isotropy to LSS [8]. What is shown here is then simply another parametrisation of the same result, but one which can bring some insight into the physics behind it. For instance, it may be that there is a bias, or systematic effect which causes the dipole and/or the quadrupole to have a surprisingly low power — such an effect could arise due to an excess on the galactic plane, for example.

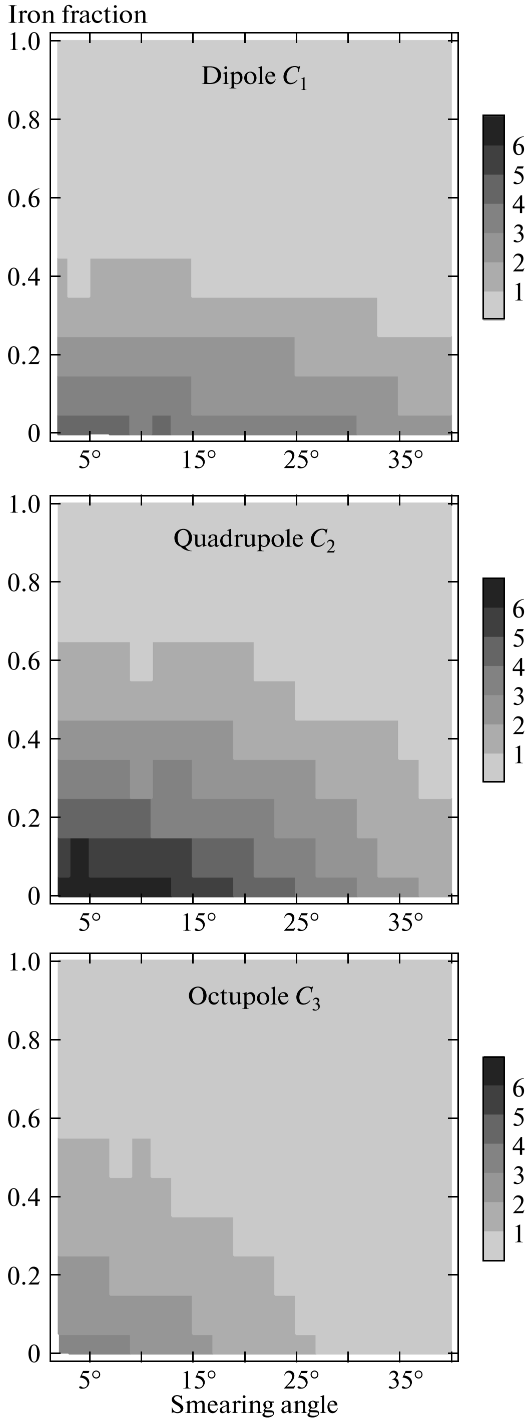

Fig. 3. Dipole, quadrupole, and octupole against LSS expectations for varying iron fraction and turbulent GMF — no regular GMF (color online see arXiv:1411.2486)

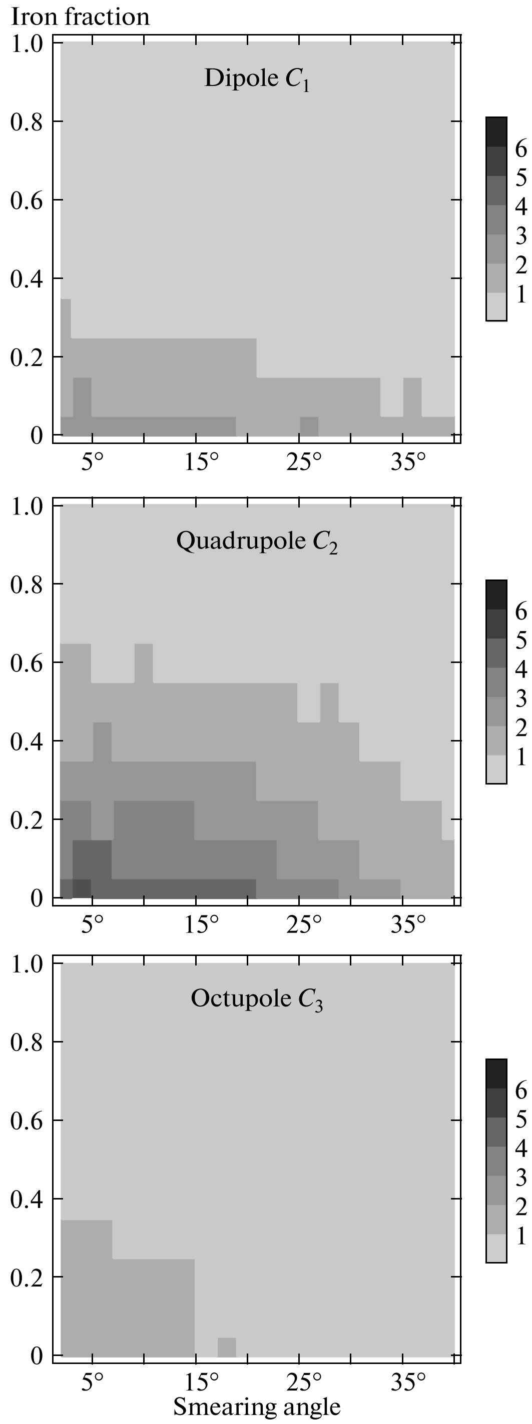

Fig. 4. Dipole, quadrupole, and octupole against LSS expectations for varying iron fraction and turbulent GMF – with regular GMF (color online see arXiv:1411.2486)

It would be extremely interesting to be able to look at the same figures above, say, 60 EeV, where instead an isotropic flux is incompatible with TA data at more than 3σ at not too large smearing angles [8]; the same data are more in line with the predictions from LSS. Unfortunately, the very low statistics in the common band of the two experiments (and consequently, large errors) makes this task quite futile at present.

Finally, as expected, the random GMF, mimicked through the smearing angle, does not affect the low-ℓ part of the power spectrum significantly — only at large smearing angles features tend to be blurred, so the differences between the LSS flux and an isotropic one are diluted.

6. CONCLUSION

For the first time, we have a full sky map of UHECRs; this opens up the possibility to decompose the flux on the sphere in a harmonic basis, and obtain its angular power spectrum C_ℓ, which is shown in Fig. 1. We wanted to see whether, in this language, a source distribution which traces that of matter (galaxies), would produce the same C_ℓ.

We find that, assuming lone proton primaries, and discarding for now the GMF, this is not the case. In particular, LSS models tend to generate a much larger power that what is extracted from the data, especially at low multipoles such as the dipole and quadrupole; the experimental full sky map is much more isotropic. The discrepancy for the quadrupole C_2 can be as strong as about 6σ, while in the case of the dipole C_1 at small smearing angles the data value is 4σ away from the LSS prediction for it.

When we turn on the regular GMF, we observe a strong correlation between the variability of the $a_{\ell m}$ values and the strength and shape of the GMF; at the same time, the power spectrum C_ℓ is much more stable against the same perturbations. The latter is therefore a more reliable observable in investigations like the one we present here. This also means that the incompatibility between data and LSS is *not* an artefact of ignoring the GMF.

Since the data prefers a more isotropic Universe, one possibility is that the primaries are heavy, and diffuse in the GMF (both regular and random). We introduced heavy nuclei in our study in the guise of a variable, isotropic fraction of the total cosmic ray flux to understand how much more isotropic distribution of UHECRs sources needs to be: in some cases (quadrupole at small and intermediate smearing angles) to tame the LSS prediction, the one may need up to about 50% or more of isotropic flux fraction.

In fact, since our method simply discriminates between an anisotropic proton flux and an isotropic one, alternative explanations are possible, not related to the composition of the primaries. An additional isotropic component may be the result of acceleration mechanisms operative away from galaxies; alternatively, the more isotropic distant sources may be contributing more than expected (for instance, due to exotic particle interactions); one more possibility is that our Galaxy is plunged into a strong magnetic wind, which isotropises the arrival directions of UHECRs even before they reach the Milky Way.

At 10 EeV, the energy threshold of the datasets we used in this work, the outcome of our analysis are not a surprise, as the data are known to be incompatible with LSS models; the multipolar description of the same result (but now with data from the full sky) can help in identifying the physical reason behind it: for instance, the C_1 and C_2 results may be signalling the presence of some systematic effect. On the other hand, the 60 EeV data does prefer LSS: it would be extremely useful to be able to repeat our exercise at those energies, but with current data this would be inconclusive. In the future, the source of these discrepancies could be identified, and it will bring some crucial insight into the hunt for UHECRs sources.

This paper has been prepared for a special volume dedicated to V. Rubakov's 60th anniversary. We seize this opportunity to wish him — a teacher and an old friend for P. T. and a colleague for F. U. — many more fruitful and happy years.

The authors are supported by IISN project No. 4.4502.13 and Belgian Science Policy under IAP VII/37. One of the authors (P. T.) is supported in part by the RFBR grant 13-02-12175-ofi-m.

APPENDIX

The flux $\Phi(\mathbf{n})$ distribution on the sphere can be projected on the right ascension plane and expanded in a Fourier series on the circle:

$$\frac{1}{2}\int d\cos\theta\,\Phi(\theta,\phi) \equiv \sum_n c_n Y_n(\phi),$$

whence

$$c_n = \frac{1}{2}\int d\mathbf{n}\,\Phi(\mathbf{n}) Y_n(\phi).$$

In order to derive the relation between the projected c_n and the spherical harmonics coefficients $a_{\ell m}$, we make use of Eq. (1) and obtain

$$c_n = \frac{2^{|n|}|n|}{8}\sum_\ell \left[(-1)^{|n|} + (-1)^\ell\right] \times \\ \times a_{\ell n}\sqrt{\frac{2\ell+1}{2}\frac{(\ell-|n|)!}{(\ell+|n|)!}} \times \\ \times \frac{\Gamma[\ell/2]\,\Gamma[(\ell+|n|+1)/2]}{\Gamma[(\ell+3)/2]\,\Gamma[(\ell-|n|+2)/2]}.$$

This implies that, *if and only if* $\Phi(\mathbf{n})$ is a pure dipole plus any other $\ell \in$ even, but does not contain any $\ell \in$ odd:

$$c_{\pm 1} = \frac{\sqrt{3}\pi}{8} a_{1,\pm 1},$$

from which follows

$$\alpha = \arctan\left(\frac{c_{-1}}{c_{+1}}\right) = \arctan\left(\frac{a_{1,-1}}{a_{1,1}}\right).$$

Since in reality there will be more multipoles, this is only a first approximation to the actual result. We have checked, again up to $\ell = 20$, that in the case of our LSS models, at the level of precision we can attain with the common analysis the higher multipoles contribute below the errors, and they become, as they should, progressively unimportant.

REFERENCES

1. K. Greisen, Phys. Rev. Lett. **16**, 748 (1966).
2. G. T. Zatsepin and V. A. Kuzmin, Pis'ma v Zh. Eksp. Teor. Fiz. **4**, 114 (1966) [JETP Lett. **4**, 78 (1966)].
3. A. Aab et al., Astrophys. J. **794**(2), 172 (2014).
4. P. Sommers, Astropart. Phys. **14**, 271 (2001).
5. M. Haverkorn, *Magnetic Fields in the Milky Way*; arXiv:1406.0283.
6. T. Abu-Zayyad et al., Pierre Auger Observatory and Telescope Array: Joint Contributions to the 33rd Int. Cosmic Ray Conf. (ICRC 2013); arXiv:1310.0647.
7. H. B. J. Koers and P. Tinyakov, arXiv:0907.0121.
8. T. Abu-Zayyad et al., Astrophys. J. **757**, 26 (2012).
9. H. B. J. Koers and P. Tinyakov, JCAP **0904**, 003 (2009).

10. R. U. Abbasi, T. Abu-Zayyad, M. Allen et al., arXiv: 1002.1444.

11. P. Abreu, M. Aglietta, E. J. Ahn et al., Astropart. Phys. **34**, 627 (2011).

12. P. Abreu et al., Astrophys. J. **762**, L13 (2012).

13. M. S. Pshirkov, P. G. Tinyakov, and F. R. Urban, Month. Not. Roy. Astron. Soc. **436**, 2326 (2013).

14. M. C. Beck, A. M. Beck, R. Beck et al., arXiv: 1409.5120.

15. M. S. Pshirkov, P. G. Tinyakov, P. P. Kronberg, and K. J. Newton-McGee, Astrophys. J. **738**, 192 (2011).